Jurnal Farmasi Indonesia: Volume 18 Nomor 2 (2026)
https://doi.org/10.35617/ jfionline.v18i2.974

Hydroxycinnamic Acids from *Drynaria sparsisora* as Anti-Vibrio Agents: Integrated In Vitro and In Silico Evidence

Hesti Marliza[1,2], Fitra Perdana[3,4], Yuli Haryani[3,4], Hilwan Yuda Teruna[3,4], Rudi Hendra[3,4*]

Artikel Penelitian

[1] Doktoral Program, Jurusan Kimia, FMIPA Universitas Riau
[2] Program Studi Kimia Fakultas Kehutanan dan Sains, Universitas Lancang Kuning, Pekanbaru, Indonesia.
[3] Jurusan Kimia, FMIPA Universitas Riau, Pekanbaru, Indonesia.
[4]Centre of Biological Innovation for Regenerative and Natural Applications, Universitas Riau, Pekanbaru, Indonesia.

Korespondensi:

Rudi Hendra
rudi.hendra@lecturer.unri.ac.id

Abstract: *Drynaria sparsisora is a fern species long utilized in ethnomedicine and recognized as a source of phenolic compounds. This study aims to isolate antibacterial ingredients from D. sparsisora, evaluate their efficacy against Vibrio species, and investigate potential molecular interactions by in silico docking analysis. Dried plant material was extracted with methanol and separated by liquid–liquid partitioning followed by chromatographic purification. Two main compounds were identified and structurally characterized using UV–Vis, FTIR, and $^{1}H/^{13}C$ NMR spectroscopy. Spectroscopic measurements established the identification of the substances as ferulic acid (1) and caffeic acid (2). In vitro antibacterial activity was investigated against Vibrio alginolyticus, Vibrio parahaemolyticus, and Vibrio cholerae using a broth microdilution method to determine minimum inhibitory concentration (MIC) and minimum bactericidal concentration (MBC). Both isolated compounds displayed MIC values of 20 µg/mL and MBC values of 40 µg/mL against all tested strains, leading to an MBC/MIC ratio of 2, confirming bactericidal activity. Although chloramphenicol revealed higher efficacy (MIC 12.5 µg/mL), the separated phenylpropanoids showed consistent and repeatable suppression across all Vibrio species tested. To give mechanistic insight, molecular docking simulations were performed against three bacterial protein targets (PDB IDs: 2ZDQ, 1HNJ, and 3IL7). Both ferulic acid and caffeic acid displayed favorable binding energies and persistent interaction patterns inside the active regions of these proteins, involving hydrogen bonding and hydrophobic interactions. In selected models, docking affinities neared those of chloramphenicol, confirming the likelihood of target engagement. The multi-target binding behavior found suggests possible interference with important bacterial functions, including cell wall function, protein synthesis, and fatty acid production. Overall, the data reveal that D. sparsisora contains hydroxycinnamic acids with considerable bactericidal activity against Vibrio spp., backed by computational evidence of protein interaction. Further investigations are necessary to validate molecular targets and clarify antibacterial processes.*

Keywords: *Drynaria sparsisora; caffeic acid; ferulic acid; antibacterial; Vibrio; molecular docking.*

Abstrak: *Drynaria sparsisora* merupakan salah satu spesies paku yang digunakan secara tradisional dalam pengobatan dan diketahui mengandung metabolit fenolik. Penelitian ini bertujuan untuk mengisolasi senyawa antibakteri dari D. sparsisora, mengevaluasi aktivitasnya terhadap bakteri Vibrio, serta mengkaji potensi interaksi molekuler melalui analisis docking in silico. Bahan tanaman kering diekstraksi menggunakan metanol dan difraksinasi melalui partisi cair–cair yang dilanjutkan dengan pemurnian kromatografi. Dua senyawa utama berhasil diisolasi dan dielusidasi strukturnya menggunakan spektroskopi UV–Vis, FTIR, serta NMR ^{1}H dan ^{13}C. Data spektroskopi mengonfirmasi bahwa kedua senyawa tersebut adalah asam ferulat (Senyawa 1) dan asam kafeat (Senyawa 2). Aktivitas antibakteri in vitro diuji terhadap Vibrio alginolyticus, Vibrio parahaemolyticus, dan Vibrio cholerae menggunakan metode mikrodilusi untuk menentukan nilai minimum inhibitory concentration (MIC) dan minimum bactericidal concentration

(MBC). Kedua senyawa menunjukkan nilai MIC sebesar 20 µg/mL dan MBC sebesar 40 µg/mL terhadap seluruh strain yang diuji, dengan rasio MBC/MIC sebesar 2 yang menunjukkan sifat bakterisidal. Meskipun kloramfenikol sebagai kontrol positif menunjukkan aktivitas yang lebih kuat (MIC 12,5 µg/mL), kedua senyawa fenilpropanoid tersebut memperlihatkan aktivitas yang konsisten terhadap semua spesies Vibrio yang diuji. Untuk memberikan pemahaman mekanistik, dilakukan simulasi docking molekuler terhadap tiga target protein bakteri (PDB ID: 2ZDQ, 1HNJ, dan 3IL7). Asam ferulat dan asam kafeat menunjukkan energi ikatan yang menguntungkan serta pola interaksi stabil dalam sisi aktif protein melalui ikatan hidrogen dan interaksi hidrofobik. Pada beberapa model, afinitas docking mendekati kloramfenikol, sehingga mendukung kemungkinan terjadinya interaksi dengan target protein bakteri. Pola ikatan multi-target ini mengindikasikan potensi gangguan terhadap proses esensial bakteri seperti fungsi dinding sel, sintesis protein, dan biosintesis asam lemak. Secara keseluruhan, hasil penelitian menunjukkan bahwa D. sparsisora mengandung asam hidroksisinamat dengan aktivitas bakterisidal terhadap Vibrio spp., yang didukung oleh bukti komputasional interaksi protein. Penelitian lanjutan diperlukan untuk memvalidasi target molekuler dan menjelaskan mekanisme antibakteri secara lebih mendalam.

Kata kunci: *Drynaria sparsisora*; asam kafeat; asam ferulat; antibakteri; Vibrio; molecular docking.

Introduction

Bacterial infections remain a serious concern in pharmaceutical and biomedical sciences because to the fast escalation of antimicrobial resistance (AMR) and the stall in the discovery of novel antibacterial scaffolds (1). The decreased efficacy of traditional antibiotics against resistant infections has accelerated efforts to develop alternative lead compounds, particularly those derived from natural sources. In this context, plant secondary metabolites have gained additional attention because of their structural variety and multi-target mechanisms, which may lower the possibility of resistance development (2). Phenolic compounds, especially phenolic acids, are particularly intriguing antibacterial options as they may act through numerous mechanisms such as loss of membrane integrity, modification of oxidative stress, and inhibition of important bacterial enzymes and signaling processes (3, 4).

Among bacterial pathogens of clinical and environmental relevance, *Vibrio* spp. comprises a priority group because they are connected to seafood-borne infections, diarrheal sickness, wound infections, and outbreaks in coastal areas. Several *Vibrio* species, notably *Vibrio alginolyticus, V. parahaemolyticus,* and *V. cholerae*, have substantial consequences for public health, aquaculture sustainability, and seafood safety (5). Consequently, the identification of antibacterial drugs effective against *Vibrio* spp. is vital not only for therapeutic objectives but also for minimizing infection risks in marine settings and aquaculture production systems.

Ferns (*Pteridophytes*) constitute an underexplored reserve of bioactive secondary metabolites. The genus *Drynaria* (*Polypodiaceae*) has been shown to include several secondary metabolites, including flavonoids, steroids, phenolic compounds, and terpenoids, which may contribute to varied biological functions (6). One species of particular importance in Indonesia is *D. sparsisora* (Desv.) T. Moore, colloquially known as "*paku langlayang*" or "*simbar layangan*", an epiphytic fern typically found in swamp and heath forest environments. Morphologically, the species is distinguished by small black trichomes, a firm rhizome texture, and dimorphic leaves with a bright green abaxial surface and dark green adaxial surface. Fertile leaves typically display lobed borders, and sporangia are unevenly dispersed across fertile leaf veins. These features support its botanical identity and separation from closely related congeners (7).

Phytochemical studies reveal that *D. sparsisora* leaves contain flavonoids and steroids, whereas the rhizome includes terpenoids. These metabolite classes are typically related with pharmacological qualities such as anti-inflammatory, anticancer, antibacterial, antifungal, antiviral, antioxidant, and neuroprotective activities. Additionally, ethnomedicinal use of the rhizome has been described, including application as a compress to treat bruises and swelling and topical use for skin-related diseases (8, 9). Such traditional relevance is consistent with observations on allied *Drynaria* species (e.g., *D. quercifolia* and *D. fortunei*) that contain steroids, flavonoids (including naringin), and phenolic compounds with varied bioactivities (10). Collectively, our findings support the probability that *D. sparsisora* includes antibacterial ingredients.

However, a critical research gap remains antibacterial constituents of *D. sparsisora* have not been sufficiently elucidated using bioactivity-guided isolation, and there is limited evidence connecting specific isolated metabolites to standardized antibacterial outcomes (MIC/MBC), particularly against *Vibrio* spp. Moreover, mechanistic plausibility at the molecular level is rarely explored for Indonesian medicinal ferns, however integrative studies combining in vitro activity with in silico target interaction can strengthen translational importance. Accordingly, this study addresses the following questions: (i) which antibacterial compounds can be isolated from the bioactive fraction of *D. sparsisora* and structurally characterized using spectroscopic methods; (ii) how effective are the isolated metabolites in inhibiting (MIC) and killing (MBC) *V. alginolyticus, V. parahaemolyticus*, and *V. cholerae*; and (iii) whether the metabolites show favorable binding interactions with bacterial targets in silico. An optional working hypothesis proposes that phenolic acids from *D. sparsisora* demonstrate anti-*Vibrio* activity via interactions with key bacterial macromolecular targets. Therefore, this study attempted to isolate and discover antibacterial ingredients from D. sparsisora, evaluate their anti-Vibrio efficacy using MIC and MBC assays, and estimate binding affinities by molecular docking to support mechanistic plausibility.

Materials and Methods

Plant material collection and taxonomic authentication

The fern species *Drynaria sparsisora* (Desv.) T. Moore (Polypodiaceae) was collected from Kampar Regency, Riau Province, Indonesia. The plant material was washed thoroughly to remove adherent dirt, then dried under shade at ambient temperature to prevent thermal destruction of labile contents. The dry material was later crushed into coarse powder and stored in sealed containers until extraction. Taxonomic authentication was conducted in the Botany Laboratory, Faculty of Mathematics and Natural Sciences (FMIPA), Universitas Riau, using conventional morphological and taxonomic keys to assure correct species identification prior to phytochemical analysis.

Chemicals, reagents, and instrumentation

All solvents used for extraction and chromatography, including methanol, *n*-hexane, chloroform, and ethyl acetate, were of analytical grade. Chromatographic separation employed silica gel 60 GF254 and silica gel 60 (230–400 mesh ASTM), while thin-layer chromatography (TLC) monitoring was performed using precoated silica gel GF254 plates. Spots were visualized under UV light at 254 and 366 nm, followed by anisaldehyde spraying reagent to assist in compound detection. For antibacterial assays, Mueller–Hinton broth (MHB), Mueller–Hinton agar (MHA), and resazurin dye were used as primary microbiological media and viability indicator, while chloramphenicol was applied as the reference antibiotic. Major instruments supporting this study included a rotary evaporator, vacuum liquid chromatography (VLC) apparatus, silica gel column chromatography set-up, UV cabinet, Fisher–Johns melting point apparatus, HPLC system with UV detector, FTIR spectrophotometer, UV–Vis spectrophotometer, and $^{1}H/^{13}C$ NMR spectrometer. Microbiological procedures were supported by sterile 96-well microplates, incubators, micropipettes, and standard biosafety equipment.

Extraction and solvent fractionation

The powdered fern material (3.6 kg) was submitted to maceration extraction using methanol for 24 h, and the extraction was repeated three times to ensure exhaustive recovery of secondary metabolites. The combined methanolic filtrates were concentrated under decreased pressure at approximately 40 °C to give the crude methanol extract. The crude extract was further fractionated using liquid–liquid extraction (LLE) in a separatory funnel by progressive partitioning with solvents of increasing polarity. Partitioning was first performed using n-hexane (1:1, extract to solvent ratio) to obtain the non-polar fraction. The remaining extract layer was then treated with dichloromethane using a modified technique where water (10%) was added to promote phase separation (extract: dichloromethane:water = 1:1:10), generating the dichloromethane fraction. The extraction residue was further partitioned with ethyl acetate (1:1) to form the semi-polar fraction, while the final aqueous layer was kept as the polar fraction. Each partition stage was repeated until the solvent phase became transparent, and all fractions were evaporated to dryness under reduced pressure prior to further separation.

Isolation and purification

The dichloromethane fraction was selected for chromatographic purification due to its high secondary metabolite profile as demonstrated by TLC analysis. This fraction was submitted to vacuum liquid chromatography (VLC) following pre-adsorption onto silica gel 60 GF254 in a 1:1 (w/w) ratio to improve uniform packing and maximize separation efficiency. The sample was placed onto a VLC column (7.5 cm diameter) packed with silica gel (about 8 cm bed height), then eluted under a stepwise gradient from non-polar to polar solvents. Elution started with 100% n-hexane, followed by increasing amounts of ethyl acetate in n-hexane, advancing to 100% ethyl acetate, and eventually ethyl acetate–methanol gradients terminating in 100% methanol. Fractions were collected and pooled based on comparable TLC characteristics to provide eight major fractions (F1–F8). The VLC fraction with the most promising chromatographic profile (Fraction 5) was subjected to further purification by silica gel column chromatography utilizing incremental polarity increments of n-hexane–ethyl acetate and ethyl acetate–methanol systems. Subfractions were collected systematically and monitored by TLC until crystalline isolates were obtained, which were further purified and submitted to structural investigation.

Purity confirmation of isolated compounds

Purity of isolated compounds was originally tested by TLC to confirm the appearance of single spots under UV light and following anisaldehyde spraying, demonstrating the absence of co-eluting contaminants. Melting point analysis was undertaken using a Fisher–Johns apparatus, and isolates demonstrating sharp melting points with narrow ranges (≤2 °C) were regarded to have high purity. Further confirmation was performed using high-performance liquid chromatography (HPLC) under reversed-phase conditions employing a gradient mobile phase of acetonitrile–water (20:80) at a flow rate of 1.0 mL/min, monitored at 254 nm for 30 minutes. Isolates presenting a single dominant peak without significant shoulder peaks were regarded chromatographically pure and adequate for spectroscopic analysis.

Structural elucidation

The structures of purified isolates were revealed using a combination of UV–Vis spectroscopy, Fourier-transform infrared spectroscopy (FTIR), and nuclear magnetic resonance (NMR) spectroscopy. UV–Vis analysis was performed to determine typical chromophore absorption patterns associated with phenolic and conjugated systems. FTIR spectra were utilized to confirm functional groups, particularly hydroxyl groups, conjugated carbonyl moieties, and aromatic ring vibrations. Comprehensive ^{1}H and ^{13}C NMR spectroscopy was conducted to determine the proton and carbon skeletons of isolated compounds, enabling assignment of important resonances, coupling patterns, and substitution environments. Structural confirmation was established by comparison of spectrum characteristics with literature data, culminating in the identification of

Compound **1** as ferulic acid and Compound **2** as caffeic acid.

In vitro antibacterial assay

Antibacterial activity was investigated against *Vibrio alginolyticus* ATCC17749, *V. Parahaemolyticus* ATCC 17802, and *V. Cholerae* ATCC 39315, which were selected as typical bacterial pathogens relevant to marine infection models. Bacterial inocula were generated by refreshing cultures in Mueller–Hinton broth and correcting turbidity to an optical density of approximately 0.1 at 600 nm, equating to ~1×10^5 CFU/mL. Minimum inhibitory concentration (MIC) values were established using the resazurin-based microdilution method in sterile 96-well microplates. Each well was originally filled with Mueller–Hinton broth, followed by addition of test samples and two-fold serial dilution. Extracts were examined up to 1000 ppm, whereas isolated compounds were tested up to 200 µM. Chloramphenicol served as the positive control under comparable dilution conditions. After dilution, resazurin solution was added as a viability indicator, followed by bacterial inoculum addition. Plates were incubated at 37.5 °C for 16 h, and MIC was defined as the lowest quantity inhibiting resazurin color change, suggesting suppression of bacterial metabolism. Minimum bactericidal concentration (MBC) was further established by subculturing aliquots from MIC wells onto Mueller–Hinton agar plates, followed by incubation for 16 h at 37.5 °C. The MBC was reported as the lowest concentration at which no visible bacterial colonies grew on agar plates, suggesting bactericidal action (11).

In silico antibacterial evaluation

Computational antibacterial evaluation was performed using molecular docking to predict the binding affinities and interaction patterns of the isolated drugs against selected bacterial target proteins. Ligand structures of caffeic acid and ferulic acid were designed and prepared using ChemDraw Professional 15.0, followed by conversion into three-dimensional conformations and geometry optimization prior to docking. Prepared ligands were exported into AutoDock-compatible formats to produce ligand libraries for docking simulation. Protein targets were collected from the Protein Data Bank (PDB), specifically PDB IDs 2ZDQ, 1HNJ, and 3IL7, indicating bacterial targets engaged in critical activities including cell wall-related function, protein synthesis, and fatty acid biosynthesis (KAS III), respectively. Proteins were processed using Discovery Studio Visualizer (BIOVIA) to remove superfluous components, enhance structural integrity, and define docking areas. Docking simulations were performed using AutoDock Vina, and binding affinity values (ΔG, kcal/mol) were recorded to rank ligand–protein interactions. The docked complexes were further investigated to examine critical stabilizing interactions such as hydrogen bonding and hydrophobic contacts, with chloramphenicol used as a reference comparator in the docking method (12).

Results and Discussion

Extraction and Solvent Partitioning

The powdered of *D. sparsisora* (3.6 kg) obtained from Kampar Regency, Riau Province, Indonesia, was extracted by repeated maceration using methanol (24 h × 3 cycles). Methanol was selected because of its advantageous physicochemical features for comprehensive extraction of secondary metabolites across a broad polarity spectrum, particularly phenolic acids and phenylpropanoids. As a polar protic solvent, methanol efficiently breaks plant cell walls and increases diffusion of intracellular metabolites into the solvent phase, resulting in enhanced extraction yield compared with less polar solvents. In addition, methanol is extensively employed in natural product research as a first-line extraction solvent since it solubilises both free phenolics and moderately polar conjugates, giving access to bioactivity-relevant chemical classes during early-stage screening and fractionation. This extraction strategy was also considered chemically appropriate for *Drynaria* species, which are documented to contain caffeic- and ferulic-acid derivatives as prominent constituents in ethanol-based extracts of *D. rhizoma* (e.g., 70% ethanol), suggesting that polar extraction systems are optimal for recovering these phenylpropanoid scaffolds (13).

Following concentration under reduced pressure (~40 °C) to minimize thermal

degradation, the methanolic crude extract was subjected to sequential liquid–liquid extraction (LLE) using *n-hexane*, dichloromethane, ethyl acetate, and water. This procedure was designed to reduce the crude metabolite matrix and enrich discrete metabolite classes into operationally defined polarity fractions, hence enhancing chromatographic resolution in subsequent isolation. Nonpolar matrix components such as waxes, lipids, and pigments were preferentially removed into the *n-hexane* layer, which is analytically favorable because such chemicals generally produce band widening and poor chromatographic separation. dichloromethane partitioning was then employed to enrich semipolar elements, including phenylpropanoids that typically display antimicrobial properties. Importantly, use of 10% water in the chloroform partition step (extract: dichloromethane:water = 1:1:10%) was employed to promote phase separation and eliminate persistent emulsions—an issue often encountered in rhizome extracts containing polysaccharides and amphiphilic compounds. Ethyl acetate was later employed to extract intermediate-to-polar phenolics with high hydrogen-bonding ability, whereas the residual aqueous layer maintained highly polar elements, including sugars and salts. The total LLE approach thus permitted efficient chemical enrichment of the semipolar area where hydroxycinnamic acids such as caffeic acid and ferulic acid are expected to occur in their free forms.

Isolation and Purification of Secondary Metabolites

Based on TLC profiling, the chloroform fraction was selected for chromatographic purification due to its metabolite richness and the presence of well-resolved spots suggestive of separable semipolar constituents. Vacuum liquid chromatography (VLC) was chosen as the initial purification platform because it is highly efficient for processing relatively large sample amounts while maintaining sufficient resolution for phytochemical separation. Prior to loading, the extract was preadsorbed onto silica gel (1:1 w/w), a critical step that increases sample homogeneity within the stationary phase, decreases streaking, and boosts repeatability. The VLC column was eluted using a polarity-gradient solvent system beginning with 100% *n-hexane*, followed by increasing fractions of ethyl acetate, and subsequently ethyl acetate–methanol combinations up to 100% methanol. This gradient is mechanistically suitable under normal-phase conditions: fewer polar contents elute early, whereas phenolic acids and other hydrogen-bonding metabolites elute later due to higher adsorption to silica via polar interactions.

Fraction pooling was performed on the basis of TLC similarity, obtaining pooled fractions F1–F8. Pooling is an important practical step because it saves redundant processing of chemically identical fractions, reduces solvent usage, and enhances isolation efficiency. Among the pooled fractions, Fraction 5 was prioritized for further purification because it revealed discrete, bright spots at mid-range Rf values under UV detection and anisaldehyde staining, suggesting enrichment of phenolics with good chromatographic mobility. The substantial mass yield of Fraction 5 (~16 g) further supported its designation as a metabolite-enriched fraction likely to include significant elements. Such chromatographic behaviour correlates with past phytochemical studies of *Drynariae* species, where caffeic acid and ferulic acid derivatives are typically concentrated in mid-polar fractions and extracted using silica-based chromatography and further enrichment using ODS/Sephadex systems (13).

Fraction 5 (2 g) was then submitted to silica gel column chromatography (flash system) with stepwise polarity increments from *n-hexane* to *n*-hexane–ethyl acetate mixtures (10% increments), followed by ethyl acetate and ethyl acetate–methanol gradients to 100% methanol. The use of progressive polarity adjustments rather than abrupt solvent changes is chromatographically sensible, as it offers fine control over elution strength, decreases compound co-elution, and increases isolation performance for structurally related phenylpropanoids. Subfractions were gathered consistently and monitored by TLC, then consolidated into 15 merged subfractions based on TLC patterns.

Notably, two subfractions formed crystalline deposits, reflecting the existence of chemically dominating ingredients with strong lattice-forming capacity—an predicted behaviour for hydroxycinnamic acids due to extensive

intermolecular hydrogen bonding (carboxylic acid–phenolic interactions). Compound 1 was obtained from SF11 (vials 397–398) as crystals (83 mg), while Compound 2 was obtained from SF12 (vials 400–404) as crystals (73 mg). TLC examination in different visualisation modes found single spots for each isolate, strongly supporting purity. Purity was further corroborated by narrow melting point ranges (Compound 1: 172–174 °C; Compound 2: 179–181 °C), consistent with reasonably high chemical purity. HPLC chromatograms under reversed-phase conditions showed a single dominating peak for each isolate at 254 nm, suggesting their suitability for final spectroscopic characterization.

Structural Elucidation of Isolated Compounds

Compound 1 was isolated as a crystalline solid and characterized using UV–Vis, FTIR, and NMR spectroscopy. The UV–Vis spectra in methanol displayed absorption maxima at 320 nm, 234 nm, and 217 nm, which is characteristic of a cinnamic acid-type chromophore bearing an aromatic conjugated system. The band near 320 nm corresponds to π→π* transitions in an aromatic ring coupled with an α,β-unsaturated carbonyl group, characteristic of hydroxycinnamic acid derivatives. The extra bands at 234 and 217 nm show aromatic π→π* transitions and reinforce the presence of an extended conjugation system.

FTIR spectroscopy provided functional-group confirmation. A wide absorbance at 3438 cm^{-1} revealed hydroxyl stretching, consistent with phenolic and carboxylic OH groups. The absorption at 1696 cm^{-1} matched to carbonyl stretching of a carboxylic acid, whereas the band near 1617 cm^{-1} was attributed to aromatic C=C stretching mixed with conjugated alkene contributions. A signal at 1035 cm^{-1} indicated C–O stretching consistent with ether substitution, while the existence of aliphatic C–H stretching at 2968 cm^{-1} was compatible with a methoxy group. Together, these FTIR properties support a hydroxy-methoxy substituted phenylpropanoid carboxylic acid, which is consistent with ferulic acid.

The ^{1}H NMR spectra ($CDCl_3$, 500 MHz) exhibited two important olefinic doublets at δ 7.63 (1H, d, J = 15.85 Hz) and δ 6.27 (1H, d, J = 15.85 Hz), indicating H-7 and H-8 of a trans-configured cinnamoyl system. The significant coupling constant (~16 Hz) unequivocally verifies an E-geometry for the α,β-unsaturated double bond. Aromatic resonances at δ 7.07 (1H, dd, J = 7.9, 1.5 Hz), δ 7.05 (1H, d, J = 1.5 Hz), and δ 6.88 (1H, d, J = 7.95 Hz) suggested a 1,3,4-trisubstituted aromatic ring. A singlet at δ 3.91 (3H, s) corresponds to a methoxy substituent. In the ^{13}C NMR spectrum, a signal of δ 169.97 proved the carboxylic acid carbon. Oxygenated aromatic carbons were found at δ 148.52 and δ 147.39, while aromatic/olefinic carbons occurred in the anticipated region δ 109.99–126.79 and the methoxy carbon appeared at δ 55.98. Comparison of the collected data to documented ferulic acid NMR values demonstrated remarkable consistency, enabling definite identification, **table 1**.

Table 1. Comparison of ^{1}H and ^{13}C NMR data of Compound 1 with literature (Ferulic acid).

Position	Compound 1 ($CDCl_3$; 500 MHz)		Ferulic acid ($CDCl_3$; 500 MHz)	
	δC (ppm)	δH (ppm)	δC (ppm)	δH (ppm)
1	169.9	–	171.3	–
2	115.1	6.27 (1H, d, J=15.85)	114.7	6.34 (1H, d, J=15)
3	145.9	7.63 (1H, d, J=15.85)	146.8	7.75 (1H, d, J=15)
1’	126.7	–	126.6	–
2’	123.2	7.05 (1H, d, J=1.5)	123.5	7.09 (1H, d, J=2)
3’	115.1	–	114.3	–
4’	148.5	–	148.3	–
5’	147.3	6.88 (1H, d, J=7.95)	147	6.97 (1H, d, J=9)
6’	109.9	7.07 (1H, dd, J=7.9, 1.5)	109.4	7.14 (1H, dd, J=8, 2)
7’	55.9	3.91 (3H, s)	55.9	3.98 (3H, s)

Compound **2** was likewise produced as a crystalline solid and characterized similarly. The UV–Vis spectra in methanol exhibited λmax at 327 nm, consistent with a hydroxycinnamic acid chromophore. Compared to Compound 1, the bathochromic shift is chemically explainable by the absence of a methoxy group and the inclusion of an extra hydroxyl group in caffeic acid, which enhances electron donation and resonance stabilisation of the conjugated π system, hence lowering excitation energy.

FTIR examination indicated a wide absorption at 3442 cm^{-1} consistent with numerous hydroxyl groups (phenolic OH and carboxylic OH). Aromatic stretching was found around 3025 cm^{-1}. C–O stretching bands at 1220–1279 cm^{-1} and 1175 cm^{-1} supported phenolic functionalities, while an absorption near 899 cm^{-1} corresponded to aromatic out-of-plane bending vibrations typical of substituted benzene rings. This pattern supports a polyhydroxylated aromatic acid, consistent with caffeic acid.

The ^{1}H NMR spectra (DMSO-d_6, 500 MHz) displayed three downfield singlets at δ 12.12, 9.53, and 9.14, corresponding to carboxylic and phenolic hydroxyl protons, which is compatible with a catechol-type replacement. Olefinic protons emerged at δ 7.43 (d, J = 15.9 Hz) and δ 6.19 (d, J = 15.9 Hz), again indicating an E-configured α,β-unsaturated system. Aromatic resonances at δ 7.04 (d, J = 2.1 Hz), δ 6.97 (dd, J = 8.1, 2.1 Hz), and δ 6.77 (d, J = 8.1 Hz) showed a 1,3,4-trisubstituted aromatic ring. The ^{13}C NMR spectrum indicated nine carbon signals including a carboxyl carbon at δ 167.31, oxygenated aromatic carbons in the δ 144–148 range, and aromatic/olefinic carbons within δ 114–125, compatible with caffeic acid. Comparison with existing caffeic acid spectral data indicated great concordance in **table 2**.

Table 2. Comparison of ^{1}H and ^{13}C NMR data of Compound 2 with literature (Caffeic acid).

Position	Compound 2 ($CDCl_3$; 500 MHz)		Caffeic acid ($CDCl_3$; 500 MHz)	
	δC (ppm)	δH (ppm)	δC (ppm)	δH (ppm)
1	125.11	–	125.5	–
2	115.15	7.04 (1H, d, J=2.1)	115.6	7.06 (1H, d, J=2.0)
3	144.95	–	145.5	–
1’	147.33	–	148.4	–
2’	114.82	6.77 (1H, d, J=8.1)	114.7	6.77 (1H, d, J=8.0)
3’	120.7	6.97 (1H, dd, J=8.1, 2.1)	121.4	7.00 (1H, dd, J=2.0, 8.0)
4’	144	7.43 (1H, d, J=15.9)	145.1	7.49 (1H, d, J=16.0)
5’	114.51	6.19 (1H, d, J=15.9)	115	6.27 (1H, d, J=16.0)
6’	167.31	–	167	–

The finding of caffeic acid and ferulic acid in D. sparsisora coincides with the recognized chemistry of Drynariae species and confirms the chemotaxonomic hypothesis that Drynaria rhizomes are abundant in phenylpropanoids and hydroxycinnamic acid derivatives. In a classical phytochemical study of it, Liang et al. isolated nine phenolic acids from a 70% ethanol extract through a combination of silica gel, ODS, Sephadex LH-20 chromatography, and semi-preparative HPLC, confirming caffeic acid not only as a free acid but also prominently as caffeic acid 4-*O*-β-D-glucopyranoside, alongside diverse caffeoyl-type conjugates characterised by NMR (13). These findings demonstrate that caffeic acid exists in Drynaria species as both a core scaffold and as conjugated derivatives that may be concentrated in polar fractions depending on solvent and fractionation approach.

Analytically, focused HPLC–PDA quantification has established caffeic acid 4-O-β-D-glucopyranoside as a validated marker in D. fortunei rhizomes and provides quality control based on chromatographic fingerprinting (14).

This supports the broader conclusion that caffeic derivatives are not only accidental ingredients but constitute substantial chemical markers quantifiable by approved HPLC/UPLC procedures, strengthening the relevance of phenylpropanoids in chemical standardisation frameworks (15). Importantly, extraction studies on Korean *Drynariae* species show that trans-ferulic acid is extracted more efficiently into 70% ethanol compared with water, and ethanol extracts display higher antioxidant and in vitro anti-osteoporotic activity, indicating that solvent polarity strongly influences recovery of bioactivity-relevant phenolics (16). Although the present study used methanol rather than aqueous ethanol, both are polar protic solvents and hence chemically suited for extracting hydroxycinnamic acids, rationalising the effective isolation of caffeic and ferulic acids from the semipolar chromatographic region.

Drynaria species also contain caffeic-acid–derived acyl conjugates, indicating caffeic acid as a structural precursor of highly specialised metabolites. In *D. roosii*, methyl and glyceryl 12-caffeoyloxylaurates were recovered from rhizomes, revealing that caffeoylated long-chain esters are recurring *Drynaria* metabolites and further validating the biosynthetic significance of caffeic acid scaffolds in this genus. Beyond chemical occurrence, caffeic derivatives have been connected to biological effects important to Drynaria pharmacology. Bioassay-guided studies of *D. fortunei* rhizomes in an Aβ(25–35)-induced axonal atrophy model identified phenolic constituents including caffeic acid 4-*O*-glucoside, which promoted axonal elongation, suggesting that caffeic derivatives may contribute to neuroprotective actions in addition to antioxidant and osteogenic contexts reported for Drynaria extracts. Collectively, these lines of evidence contextualise the present findings by demonstrating that caffeic and ferulic acids occur across *Drynaria* species as free acids and as glycosides/esters, are detectable by validated chromatographic workflows, and are plausibly related to the broader bioactivity landscape reported for *Drynaria* species (16, 17).

In vitro antibacterial activity

The in vitro antibacterial activity of *Drynaria sparsisora* rhizome extracts and the purified compounds was assessed against three *Vibrio* species (*Vibrio alginolyticus*, *V. parahaemolyticus*, and *V. cholerae*) using a resazurin-based microdilution method, followed by minimum bactericidal concentration (MBC) determination. Standardized bacterial inocula (OD_{600}=0.1; ~1×10^5 CFU/mL) were incubated with serial dilutions of extracts and isolates, and growth inhibition was interpreted based on resazurin colour conversion after 16 h incubation. MIC values were defined as the lowest concentrations preventing metabolic conversion of the indicator, whereas MBC values were obtained by subculturing aliquots from inhibitory wells onto Mueller–Hinton agar to determine the lowest concentration causing complete bacterial killing. This combined MIC–MBC design provides improved resolution for antibacterial profiling because it distinguishes growth suppression from bactericidal effects, which is crucial for evaluating candidate antibacterial leads.

As summarised in Table 3, the crude extracts exhibited weak-to-moderate antibacterial activity against the tested *Vibrio* species, with clear dependence on extract polarity. Among all solvent fractions, the dichloromethane extract demonstrated the most favourable antibacterial profile, showing MIC values of 1000 µg/mL against *V. alginolyticus* and >1000 µg/mL against *V. parahaemolyticus* and *V. cholerae*, with MBC values >1000 µg/mL across the panel.

Table 3. MIC and MBC values of extracts and isolated compounds against *Vibrio* spp.

Sample	*V. alginolyticus*		*V. parahaemolyticus*		*V. cholerae*	
	MIC	**MBC**	**MIC**	**MBC**	**MIC**	**MBC**
Methanol extract	1000	>1000	1000	>1000	>1000	>1000
n-Hexane extract	1000	>1000	>1000	>1000	>1000	>1000
Dichloromethane extract	1000	>1000	>1000	>1000	>1000	>1000
Ethyl acetate extract	500	1000	500	>1000	1000	>1000

Water extract	>1000	>1000	>1000	>1000	>1000	>1000
Compound **1**	20	40	20	40	20	40
Compound **2**	20	40	20	40	20	40
Chloramphenicol	12.5	50	12.5	12.5	12.5	50

Although the MIC values remained in the high µg/mL range, the comparatively improved performance of the chloroform extract—relative to the n-hexane and aqueous extracts—suggests enrichment of bioactive semipolar metabolites in this fraction. This is chemically plausible because chloroform efficiently extracts mid-polar constituents such as free phenolic acids, phenylpropanoids, and less polar polyphenolic derivatives, while excluding highly polar sugars and salts that can dilute activity and complicate diffusion in aqueous assay matrices.

Notably, the ethyl acetate fraction showed MIC values of 500–1000 µg/mL against *V. alginolyticus* and *V. parahaemolyticus* (Table 3), indicating that mid-polar phenolics may also distribute into ethyl acetate, as expected.

However, given the overall fraction performance and the isolation outcomes, the data support that the bioactivity-guided prioritization towards semipolar fractions (chloroform/ethyl acetate space) was justified, and chloroform emerged as the most practically informative extract fraction for the present purification strategy. Importantly, the observation that crude extracts showed limited bactericidal potential (MBC mostly >1000 µg/mL) is consistent with typical botanical matrices, where active principles may be present at low abundance and may be partially antagonized or masked by co-extracted components.

In the context of previous literature, Drynaria rhizomes have been repeatedly reported as antibacterial sources, particularly with organic-solvent extracts. Ranjan Padhy et al. (2015) demonstrated broad-spectrum antibacterial activity of methanolic rhizome extracts of *Drynaria quercifolia*, and highlighted that in vitro-grown samples may show stronger antibacterial inhibition than in vivo samples, supporting the impact of metabolite variability and growth conditions (18). Furthermore, Ashna et al. (2023) reported ethyl acetate extracts as highly effective against several bacterial pathogens, including strong inhibition of *Bacillus subtilis* when compared with standard antibiotics. However, most available fern antibacterial studies largely focus on common Gram-positive and Gram-negative test bacteria (e.g., *E. coli*, *S. aureus*, *Bacillus* spp., *Salmonella* spp.) and rarely include *Vibrio* species, implying that antibacterial evidence against *Vibrio* remains underdeveloped and that further targeted screening is warranted (19).

Compared with the extract fractions, the purified hydroxycinnamic acids exhibited substantially stronger and more consistent antibacterial activity across the three *Vibrio* species. Both Compound 1 (ferulic acid) and Compound 2 (caffeic acid) produced MIC values of 20 µg/mL and MBC values of 40 µg/mL against *V. alginolyticus*, *V. parahaemolyticus*, and *V. cholerae* (Table 3). This clear activity enhancement after purification is expected and reinforces that the antibacterial effect is primarily driven by low-molecular-weight phenolics rather than by the bulk extract matrix. In practical terms, purification increases the relative concentration of the active pharmacophore and reduces interference by inactive constituents that may reduce apparent potency in crude extracts.

A particularly important interpretation derived from paired MIC–MBC outcomes is that both compounds can be considered bactericidal under the present experimental conditions. Specifically, the MBC/MIC ratios for both isolates were 2, which is below the widely used bactericidal threshold of 4. This interpretation aligns with the antibacterial categorization applied by Teruna et al. (2024), where compounds with MBC/MIC < 4 were considered bactericidal. The bactericidal designation strengthens the pharmacological relevance of these phenolics, as bactericidal compounds are frequently preferred for controlling invasive infections and may reduce the persistence of viable pathogens (12).

The bactericidal activity observed for caffeic acid and ferulic acid is supported by mechanistic evidence from related studies. Ferulic acid has

been shown to disrupt bacterial cell membranes, altering membrane permeability and surface charge, and resulting in irreversible membrane damage accompanied by energetic collapse such as decreased intracellular ATP, which can translate into lethal outcomes in susceptible strains. Similarly, caffeic acid has been widely discussed as an antibacterial phenolic with multi-target effects, including interference with membrane integrity, inhibition of cell wall-related processes, anti-biofilm activity, and synergy with antibiotics, suggesting potential utility in combination therapies against resistant bacteria (20). Importantly, despite abundant evidence of antibacterial activity of these hydroxycinnamic acids against major pathogens, reports against *Vibrio* spp. remain scarce, rendering the present findings relevant as an extension of phenolic antibacterial profiling into marine bacterial pathogens.

Taken together, the extract-level screening indicates that semipolar organic fractions—particularly chloroform—concentrate antibacterial constituents more effectively than highly polar or nonpolar fractions, while compound-level testing demonstrates that ferulic acid and caffeic acid are responsible for potent and bactericidal inhibition against *Vibrio* spp. These results support bioassay-guided purification as a rational strategy for identifying active principles from Drynaria rhizomes and provide a mechanistic foundation for further studies, including synergy assays, membrane integrity evaluation, and molecular docking interpretation.

In Silico Antibacterial Activity

To complement the in vitro antibacterial findings and provide mechanistic plausibility at the molecular level, molecular docking simulations were conducted to evaluate the binding potential of the isolated compounds—Compound 1 (ferulic acid) and Compound **2** (caffeic acid)—against three bacterial protein targets (PDB IDs: 2ZDQ, 1HNJ, and 3IL7). These targets were selected to represent critical bacterial physiological activities, including cell wall-associated function (2ZDQ), protein synthesis-related activity (1HNJ), and fatty acid biosynthesis initiation via β-ketoacyl-acyl carrier protein synthase III (KAS III) (3IL7). Chloramphenicol was used as a positive control antibiotic to establish a pharmacological benchmark for comparing binding performance. Docking simulations were performed using AutoDock Vina, following typical preparation processes comprising removal of crystallographic water molecules and heteroatoms, insertion of polar hydrogens, assignment of Gasteiger charges, and energy minimization of ligand conformations. Predicted binding free energies (ΔG, kcal/mol) were determined for each ligand–target pair and are reported in Table 4, while ligand binding orientations within the protein pockets are displayed in Figures 2–4.

Table 4. Comparative molecular docking results for three targets (2ZDQ, 1HNJ, and 3IL7).

Com-pound	2ZDQ ΔG (kcal/mol)	2ZDQ H-bond residues	2ZDQ Hydrophobic residues	1HNJ ΔG (kcal/mol)	1HNJ H-bond residues	1HNJ Hydrophobic residues	3IL7 ΔG (kcal/mol)	3IL7 H-bond residues	3IL7 Hydrophobic residues
1	-7.8	LEU192 ALA191	PHE151 PHE272	-6.1	ALA246 GLY305	ALA246	-5.7	ASN268 HIS238	LEU156 MET201 VAL206
2	-7.5	LEU192	PHE151 ILE163	-6.2	ASN247 ASN274 GLY209 PHE304	CYS112 LEU189 MET027 PHE157 VAL212	-5.9	SER152	TRP32

Chloramphenicol	-7.9	ASN281	PHE151 PHE222	-6.6	ASN247 ASN274 ALA246 GLY209	ALA216 ALA246 ALA246 ILE156	-6.0	CYS112 GLY300	ALA81 LEU190 LEU199

Table 4 reveals that both hydroxycinnamic acids showed favorable predicted binding across all three sites, with docking energies approaching those of chloramphenicol. For 2ZDQ, chloramphenicol showed the most favorable binding energy (ΔG = −7.9 kcal/mol), closely followed by caffeic acid (ΔG = −7.8 kcal/mol) and ferulic acid (ΔG = −7.5 kcal/mol). This implies that caffeic acid, in particular, displays binding affinity roughly similar to the clinically optimized antibiotic within the 2ZDQ active region.

For 1HNJ, chloramphenicol again revealed the lowest ΔG (−6.6 kcal/mol), whilst caffeic acid (−6.1 kcal/mol) and ferulic acid (−6.2 kcal/mol) showed relatively weaker but consistent interactions. In 3IL7 (KAS III), the binding energy differences were smaller: chloramphenicol demonstrated ΔG = −6.0 kcal/mol, while ferulic acid and caffeic acid yielded −5.9 and −5.7 kcal/mol, respectively. The relative proximity of ferulic acid to chloramphenicol in this target suggests particularly favorable geometric compatibility with the KAS III binding pocket.

Docking interpretation must involve not only ΔG measurements but also the interaction networks. Hydrogen bonding contributes to binding selectivity and catalytic anchoring, while hydrophobic and π-interactions support ligand location within the binding cavity. Caffeic acid, carrying a catechol moiety (two phenolic hydroxyl groups) and a terminal carboxyl group, has various hydrogen bond donor–acceptor properties. Ferulic acid, with one phenolic hydroxyl and one methoxy group, produces fewer hydrogen bonds but compensates through hydrophobic packing and aromatic interactions. Chloramphenicol, by contrast, has many heteroatoms and functional groups, providing a denser and more diversified interaction network, which explains its continuously greater docking energies.

In the 2ZDQ target, caffeic acid obtained ΔG = −7.8 kcal/mol, virtually matching chloramphenicol (−7.9 kcal/mol), as indicated in Table 4. This shows good binding compatibility inside the 2ZDQ pocket. Caffeic acid established hydrogen connections with LEU192 and ALA191, while hydrophobic stabilization occurred through interactions with PHE151 and PHE272. The phenylalanine residues contribute π–π stacking and π–alkyl interactions with the aromatic ring of caffeic acid, while hydrogen bonding via the catechol and carboxyl groups maintains appropriate ligand orientation.

Ferulic acid displayed slightly poorer binding (ΔG = −7.5 kcal/mol), establishing hydrogen bonding with LEU192 and hydrophobic interactions with PHE151 and ILE163. The reduced hydrogen bonding is consistent with its lower polarity relative to caffeic acid. However, the methoxy group promotes hydrophobic complementarity inside the semi-polar binding pocket.Chloramphenicol displayed ΔG = −7.9 kcal/mol and formed a hydrogen bond with ASN281, alongside hydrophobic interactions with PHE151 and PHE222. The strong interaction network correlates with its recognized antibacterial effectiveness.

Figure 1 gives a three-dimensional depiction of these interactions, indicating that caffeic acid and ferulic acid occupy overlapping portions of the 2ZDQ binding cavity comparable to chloramphenicol. This spatial overlap suggests potential competitive binding within a functionally significant location and underscores the role of aromatic residues in stabilizing phenylpropanoid ligands. For 1HNJ, chloramphenicol demonstrated the most favorable binding energy (−6.6 kcal/mol), consistent with its activity as a protein synthesis inhibitor. Hydrogen bonds were established with ASN247, ASN274, ALA246, and GLY209, while hydrophobic stabilization implicated ALA246 and ILE156, showing high complementarity within the binding area.

Caffeic acid displayed ΔG = −6.1 kcal/mol and formed hydrogen bonds with ALA246 and GLY305, with hydrophobic stabilization predominantly involving ALA246. Although weaker than chloramphenicol, the engagement of critical residues shows that caffeic acid occupies a functionally significant binding area. Ferulic acid generated ΔG = −6.2 kcal/mol and formed hydrogen bonds with ASN247, ASN274, GLY209, and PHE304, along with significant hydrophobic interactions including CYS112, LEU189, MET027, PHE157, VAL212, ALA216, and ALA246. This wider hydrophobic interaction network suggests deeper penetration into the pocket, potentially compensating for diminished hydrogen-bonding capabilities.

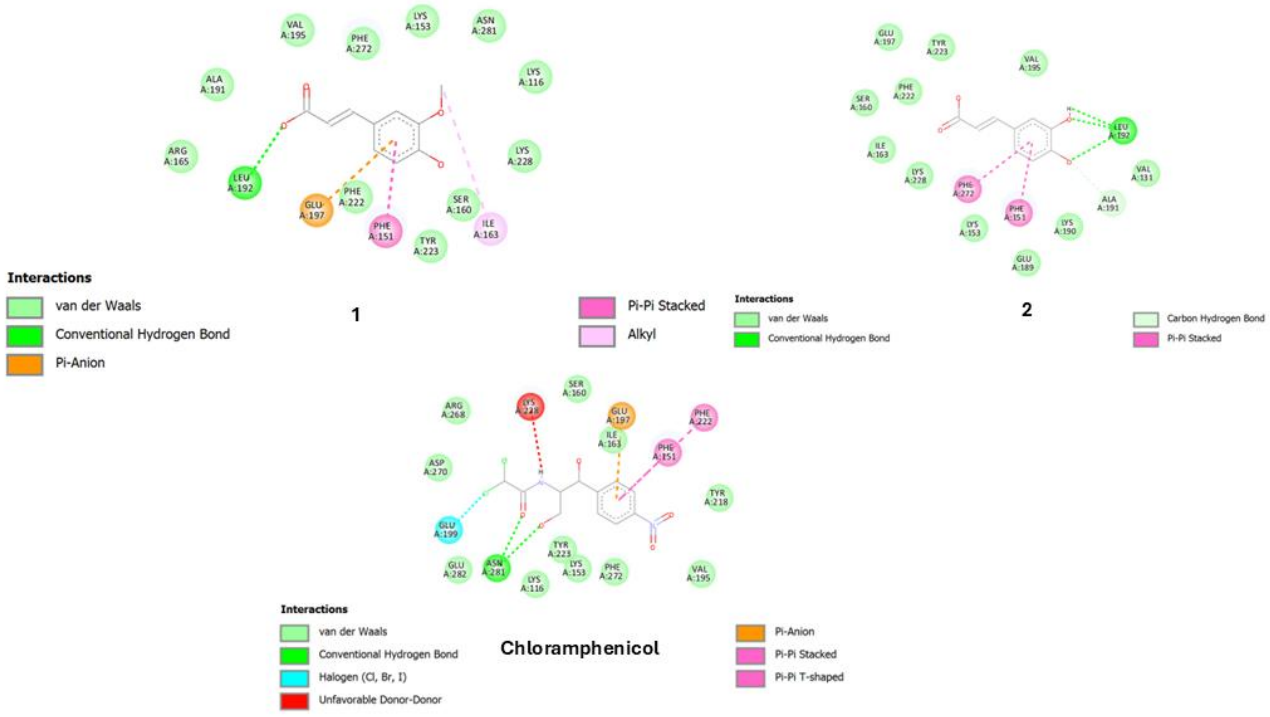

Figure 1. Spatial arrangement of compounds with protein target (PDB ID; 2ZDQ).

Figure 2 visualizes these binding states and reveals that both hydroxycinnamic acids assume stable postures within the 1HNJ pocket. The overlap with chloramphenicol's binding area shows that although these natural chemicals are structurally simpler, they may nonetheless interfere with protein synthesis-related processes. The 3IL7 target corresponds to β-ketoacyl-acyl carrier protein synthase III (KAS III), a key enzyme starting fatty acid biosynthesis. Because fatty acid synthesis is important for membrane production and bacterial growth, blockage of KAS III is a recognized antibacterial approach. Chloramphenicol revealed ΔG = −6.0 kcal/mol, while ferulic acid and caffeic acid demonstrated −5.9 and −5.7 kcal/mol, respectively (Table 4). The little difference between ferulic acid and chloramphenicol shows particularly excellent compatibility of ferulic acid within the KAS III pocket. Caffeic acid produced hydrogen connections with ASN268 and HIS238 and hydrophobic interactions with LEU156, MET201, and VAL206. Ferulic acid produced hydrogen bonding with SER152 and hydrophobic contact with TRP32. Chloramphenicol engaged via hydrogen bonds with CYS112 and GLY300, amid hydrophobic interactions with ALA81, LEU190, and LEU199.

Figure 3 indicates that both phenylpropanoids occupy stabilizing orientations

https://doi.org/10.35617/ jfionline.v18i2.974

within the catalytic domain of KAS III, supporting the notion that interfering with fatty acid production may contribute to antibacterial action. Given that membrane biosynthesis is crucial for viability, such suppression may synergize with membrane-disruptive actions typical of phenolic acids. The docking results (Table 4; Figures 2–4) support the in vitro findings, in which both caffeic acid and ferulic acid displayed MIC = 100 µg/mL and MBC = 200 µg/mL against Vibrio spp., with MBC/MIC = 2 showing bactericidal action. The multi-target binding pattern found in docking shows that antibacterial effects may not rely on a single enzymatic route but rather on simultaneous interference with cell wall-associated proteins (2ZDQ), protein synthesis-related targets (1HNJ), and fatty acid biosynthesis (3IL7).

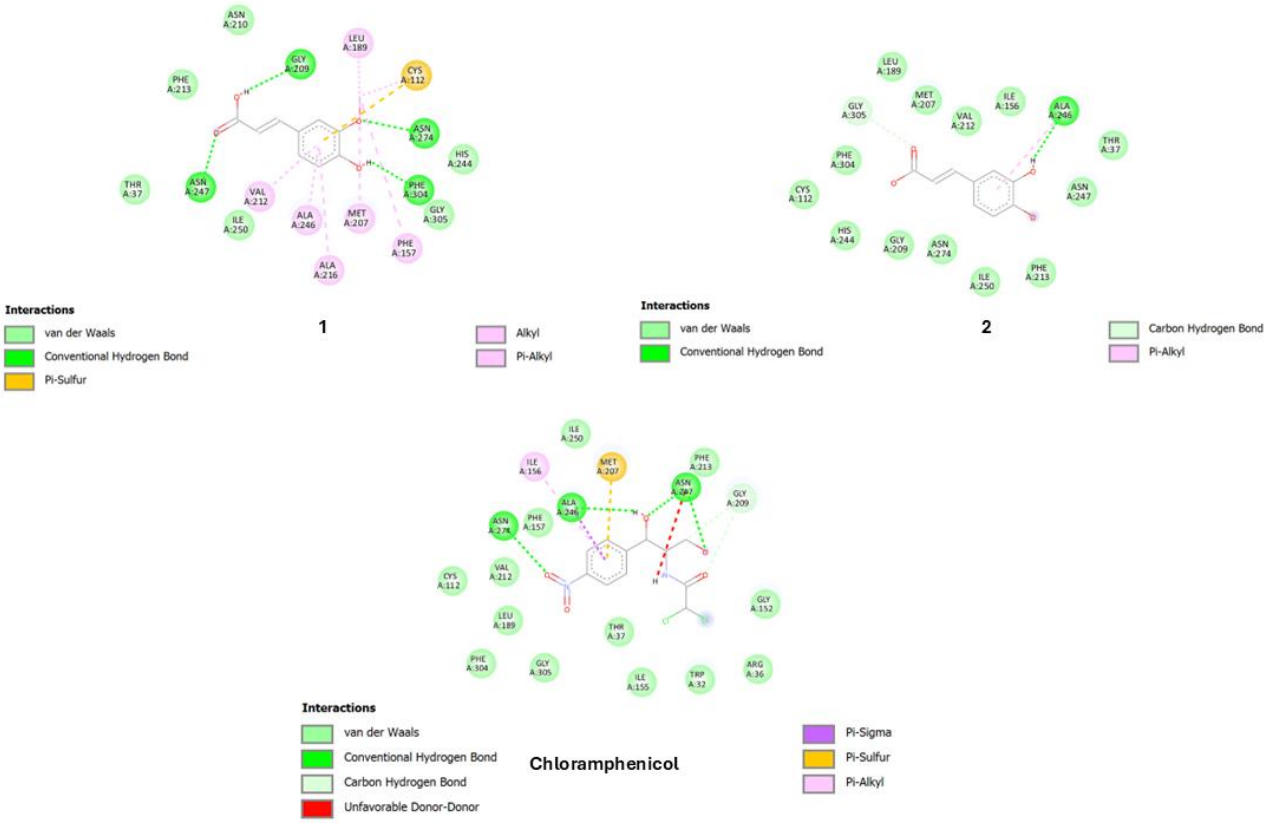

Figure 2. Spatial arrangement of compounds with protein target (PDB ID; 1HNJ).

This interpretation corresponds with broader literature. Bhattacharya et al. (2025) showed that caffeic acid has broad-spectrum antibacterial activity supported by in silico, in vitro, and in vivo evidence, including anti-biofilm, anti-quorum sensing, and efflux pump inhibitory mechanisms (21). Similarly, Umaarasu et al. (2018) reported that ferulic acid displayed docking energies comparable to cefotaxime against β-lactamase enzymes (22). Vaikkathillam et al. (2025) revealed antibiofilm activity of ferulic acid supported by docking and molecular dynamics investigations (23). Abu-Qatouseh et al. (2025) also found that ferulic acid impacts gene expression linked with virulence and metabolism in *Helicobacter pylori* (24).

Collectively, these data increase the mechanistic plausibility that docking-predicted binding reflects actual antibacterial potential rather than computational artifact. A remarkable part of this work is its focus on Vibrio species, for which phenylpropanoid antibacterial evidence remains sparse. While caffeic and ferulic acids have been widely researched against common Gram-positive and Gram-negative bacteria, specific findings against *Vibrio* are limited.

Therefore, the combined in vitro bactericidal data and supported docking outcomes provide a solid molecular.

Conclusion

This study successfully isolated and identified ferulic acid and caffeic acid from *D. spars*a nd proved their bactericidal action against *Vibrio alginolyticus, V. parahaemolyticus,* and *V. cholerae*. Both compounds displayed consistent MIC and MBC values, showing measurable antibacterial effectiveness, but lower than chloramphenicol. Molecular docking validated these findings by establishing stable binding contacts with bacterial targets (2ZDQ, 1HNJ, and 3IL7), suggesting potential multi-target engagement. While more mechanistic validation is necessary, the results show that hydroxycinnamic acids from *D. sparsisora* contribute to its antibacterial properties and deserve continuing exploration as natural antibacterial scaffolds.

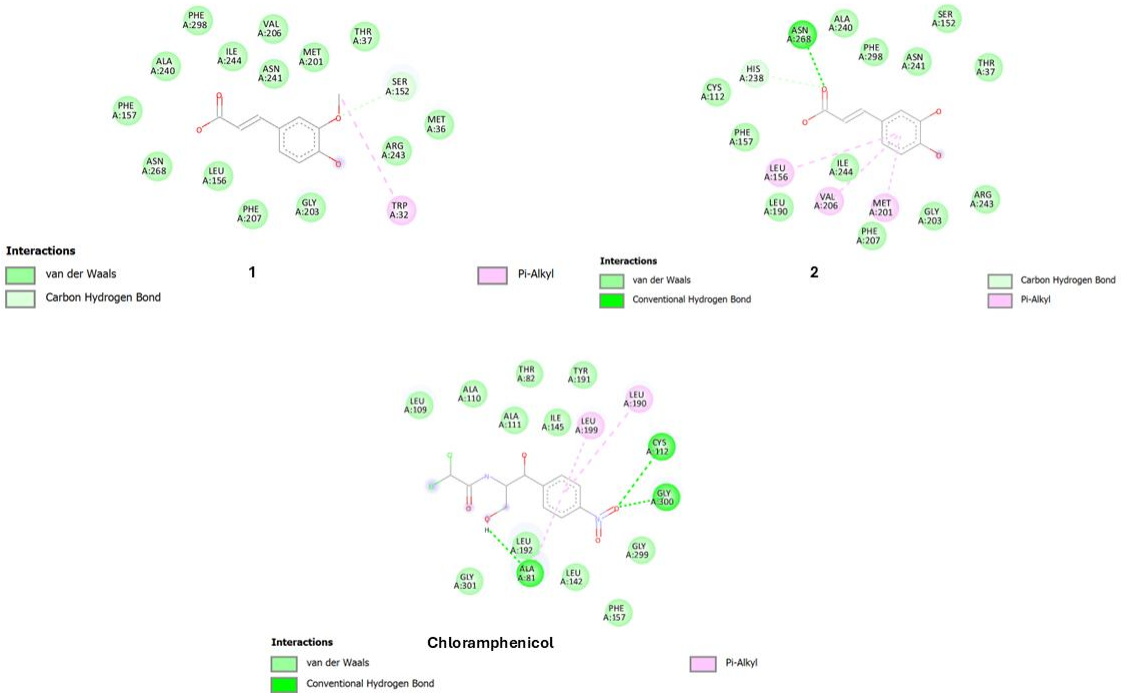

Figure 3. Spatial arrangement of compounds with protein target (PDB ID; PDB 3IL7).

Acknowledgement

The Directorate of Research and Community Service, Ministry of Higher Education, Science, and Technology, Republic of Indonesia, provided financial assistance for this project under contract number 102/C3/DT.05.00/PL/2025. The authors further express their heartfelt gratitude to the Institute for Research and Community Service, Universitas Riau, for their ongoing assistance and facilitation during the duration of this research.

Disclosure Statement

The authors disclose no competing interests, whether financial or non-financial, with this work.

References

1. Iskandar K, Murugaiyan J, Hammoudi Halat D, Hage SE, Chibabhai V, Adukkadukkam S, et al. Antibiotic discovery and resistance: the chase and the race. Antibiotics. 2022;11(2):182.
2. Rafeeq A, Arshad S, Abid MA, Sajjad MA, Shahzad M, Qadir ML, et al. Potential of Plant-Derived Phytochemicals in

Combating Antimicrobial Resistance: A Comprehensive Review. Journal of Health, Wellness and Community Research. 2025:e762-e.
3. Ahluwalia V, Nusrat I, Samsul A, Vinod K, Thakur L, Jitendra K. Recent advancement in polyphenols as potential antibacterial agents: a comprehensive review. Current Chinese Chemistry. 2021;1(2).
4. Lobiuc A, Pavăl N-E, Mangalagiu II, Gheorghiță R, Teliban G-C, Amăriucăi-Mantu D, et al. Future antimicrobials: Natural and functionalized phenolics. Molecules. 2023;28(3):1114.
5. Loo K-Y, Law JW-F, Tan LT-H, Pusparajah P, Wong SH, Chan K-G, et al. The burden of Vibrio sp. infections–A scoping review. Progress In Microbes & Molecular Biology. 2023;6(1).
6. Jingying G, Yonghong L, Huawei F, Huilian H, Jianqun L, Caiying P, et al. A comprehensive review of Drynariae rhizoma: botany, traditional applications, and active flavonoid components. J Pharm Pharmacol. 2025;77(10):1319-37.
7. Majid A, Ajizah A, Amintarti S. Keragaman tumbuhan paku (pteridophyta) di taman biodiversitas hutan hujan tropis mandiangin. Jurnal Al-Azhar Indonesia Seri Sains Dan Teknologi. 2022;7(2):102-12.
8. Mani K, Aiyalu R, Thiruvengadarajan V, Arivukkarasu R, Suriyapriya K. A Comprehensive Review of Drynaria quercifolia (L.) J. Sm. Pharmacognosy Reviews. 2023;17(34).
9. Deepa N, Nirmala S, Yogalakshmi T, Udhayakumaran U, Velvizhi K. Phytochemistry, Traditional Applications, and Therapeutic Properties of Drynaria quercifolia. Journal of Pharma Insights and Research. 2025;3(3):379-91.
10. Sujin RM, Jeeva S, Subin RM. Phytochemical and pharmacological studies of oak leaf fern, Drynaria quercifolia (L.) J. Sm: A review. The Phytochemical and Pharmacological Aspects of Ethnomedicinal Plants. 2021:373-87.
11. Army MK, Khodijah R, Haryani Y, Teruna HY, Hendra R. Antibacterial *in vitro* screening of Helminthostachys zeylanica (L.) Hook. root extracts. J pharm pharmacogn res. 2023;11(2):291-6.
12. Teruna HY, Khodijah R, Frimayanti N, Hendra R. Phytochemicals from Pyrrosia longifolia (Burm. f.) C.V. Morton with Antibacterial Activity. Research in Pharmaceutical Sciences. 2024;19(3):712-28.
13. Liang Y, Ye M, Zhang L, Li H, Han J, Wang B, et al. Two new phenolic acids from Drynariae Rhizoma. Yao xue xue bao= Acta Pharmaceutica Sinica. 2010;45(7):874-8.
14. Liu H, Zou S, Qi Y, Zhu Y, Li X, Zhang B. Quantitative determination of four compounds and fingerprint analysis in the rhizomes of Drynaria fortunei (Kunze) J. Sm. Journal of natural medicines. 2012;66(2):413-9.
15. Ahn JS, Whang WK. The Development and Validation of Simultaneous Multi-Component Quantitative Analysis via HPLC–PDA Detection of 12 Secondary Metabolites Isolated from Drynariae Rhizoma. Separations. 2023;10(12):601.
16. Kang S-N, Lee JS, Park J-H, Cho J-H, Park J-H, Cho K-K, et al. In vitro anti-osteoporosis properties of diverse Korean Drynariae rhizoma phenolic extracts. Nutrients. 2014;6(4):1737-51.
17. Wufuer H, Xu Y, Wu D, He W, Wang D, Zhu W, et al. Liglaurates A–E, cytotoxic bis (lauric acid-12yl) lignanoates from the rhizomes of Drynaria roosii Nakaike. Phytochemistry. 2022;198:113143.
18. Padhy R, Dash SK. Antibacterial evaluation of methanolic Rhizome extract from an in vivo and in vitro grown Pteridophyte, Drynaria quercifolia (Linn.) J. Smith. Asian J Pharm Clin Res. 2015;8(4):130-8.
19. Ashna T, Joy LM, Antony S, Sindu T, Mol S, Shiji T, et al. In vitro anti-bacterial screening of drynariya quercifolia. Journal of Innovations in Applied Pharmaceutical Science (JIAPS). 2023:120-3.
20. Shi C, Zhang X, Sun Y, Yang M, Song K, Zheng Z, et al. Antimicrobial activity of ferulic acid against Cronobacter sakazakii and possible mechanism of action. Foodborne pathogens and disease. 2016;13(4):196-204.

21. Bhattacharya M, Mandal S. Antibacterial activity of caffeic acid from plant sources: A review based on in silico, in vitro and in vivo approaches. The Microbe. 2025:100541.
22. Umaarasu T, Padmavathy K, Thirunavukkarasu D, Sv R, Shanmugam G. Molecular docking studies of Ricinus communis phytochemicals against beta-lactamase from Enterococcus faecalis and Staphylococcus aureus. Asian J Pharm Clin Res. 2018;11(7):132-7.
23. Vaikkathillam P, Mini M, Mohan A, Jayakumar D, Rajan PP, Asha S, et al. Anti-biofilm effect of ferulic acid against Enterobacter hormaechei and Klebsiella pneumoniae: in vitro and in silico investigation. Biofouling. 2025;41(2):157-70.
24. Abu-Qatouseh LF, Ahmad MI, Amorim CG, Al-Adham IS, Collier PJ, Montenegro MC. Insights into the molecular antimicrobial properties of ferulic acid against Helicobacter pylori. J Appl Microbiol. 2025;136(5):lxaf112.